

NEW COMPLEXITY BOUNDS FOR PRIMAL–DUAL INTERIOR-POINT ALGORITHMS IN CONIC OPTIMIZATION

JOACHIM DAHL, LEVENT TUNÇEL, AND LIEVEN VANDENBERGHE

ABSTRACT. We provide improved complexity results for symmetric primal–dual interior-point algorithms in conic optimization. The results follow from new uniform bounds on a key complexity measure for primal–dual metrics at pairs of primal and dual points. The complexity measure is defined as the largest eigenvalue of the product of the Hessians of the primal and dual barrier functions, normalized by the proximity of the points to the central path. For algorithms based on self-scaled barriers for symmetric cones, we determine the exact value of the complexity measure. In the significantly more general case of self-concordant barriers with negative curvature, we provide the asymptotically tight upper bound of $4/3$. This result implies $O(\vartheta^{1/2} \ln(1/\epsilon))$ iteration complexity for a variety of symmetric (and some nonsymmetric) primal–dual interior-point algorithms. Finally, in the case of general self-concordant barriers, we give improved bounds for some variants of the complexity measure.

1. INTRODUCTION

Primal–dual algorithms are among the most efficient, both in theory and in practice, and most robust algorithms for convex optimization. Primal–dual scalings (metrics) play a key role in the primal–dual algorithms, including interior-point algorithms. In this paper, we provide new bounds on complexity measures for primal–dual scalings. The new bounds directly yield iteration complexity upper bounds for a class of primal–dual interior-point algorithms.

Let $K \subset \mathbb{R}^n$ be a pointed, closed, and convex cone with nonempty interior. We call such cones *regular*. If K is a regular cone, then so is the dual cone

$$K^* := \{s \in \mathbb{R}^n : \langle s, x \rangle \geq 0 \text{ for all } x \in K\}. \quad (1)$$

Given a linear transformation $A : \mathbb{R}^n \rightarrow \mathbb{R}^m$, $b \in \mathbb{R}^m$, $c \in \mathbb{R}^n$, we define a conic optimization problem as

$$\begin{aligned} & \text{minimize} && \langle c, x \rangle \\ & \text{subject to} && A(x) = b \\ & && x \in K, \end{aligned} \quad (\text{P})$$

Date: September 9, 2025.

Joachim Dahl: Cardinal Operations, Ltd., China (e-mail: dahl.joachim@gmail.com).

Levent Tunçel: Department of Combinatorics and Optimization, Faculty of Mathematics, University of Waterloo, Waterloo, Ontario N2L 3G1, Canada (e-mail: levent.tuncel@uwaterloo.ca). Research of this author was supported in part by Discovery Grants from NSERC and by U.S. Office of Naval Research under award number N00014-18-1-2078.

Lieven Vandenberghe: Department of Electrical and Computer Engineering, UCLA, Los Angeles, CA 90095, USA (e-mail: vandenbe@ucla.edu).

with variable $x \in \mathbb{R}^n$. The dual problem is defined as

$$\begin{aligned} & \text{maximize} && b^\top y \\ & \text{subject to} && A^*(y) + s = c \\ & && s \in K^*, \end{aligned} \tag{D}$$

with variables $y \in \mathbb{R}^m$, $s \in \mathbb{R}^n$, where the linear transformation $A^* : \mathbb{R}^m \rightarrow \mathbb{R}^n$ (the *adjoint* of A) is defined by the identity

$$\langle A^*(y), x \rangle = y^\top A(x), \quad \forall x \in \mathbb{R}^n, \quad \forall y \in \mathbb{R}^m.$$

Algorithms which simultaneously solve (P) and (D) by generating a sequence of primal–dual iterates $x^{(k)} \in \text{int}(K)$ and $s^{(k)} \in \text{int}(K^*)$ are relevant to this paper. Among such algorithms, we focus on those which can be interpreted as using a variable primal–dual scaling in each iteration. Specifically, a scaling is a symmetric positive definite matrix $T^{(k)}$ used in the equations

$$A(d_x) = 0, \quad A^*(d_y) + d_s = 0, \quad T^{(k)}d_x + d_s = r,$$

which determine the primal and dual search directions d_x, d_y, d_s at iteration k . Primal–dual scalings are also known as primal–dual metrics because of their close connections with variable metric methods in the optimization literature including the usage of variable metrics in quasi-Newton methods.

The scaling used in primal–dual interior-point methods for linear programming (with $K = \mathbb{R}_+^n$) is the diagonal matrix with diagonal entries $T_{ii}^{(k)} = s_i^{(k)} / x_i^{(k)}$; see [37]. For semidefinite and second-order cone programming, a wide variety of scalings which generalize the primal–dual scaling for $K = \mathbb{R}_+^n$ have been studied and used successfully (see, for instance [32] and the references therein). The most complete theory for primal–dual scalings is the theory of *self-scaled barriers* due to Nesterov and Todd [19, 20], which covers the cases when the cone K is the nonnegative orthant, \mathbb{R}_+^n , the cone of symmetric positive semidefinite matrices over reals, \mathbb{S}_+^n , the cone of Hermitian positive semidefinite matrices over complex numbers, \mathbb{H}_+^n , and the direct sum (or cartesian product) of second order cones. More precisely, the theory of self-scaled barriers treats the cases when K is a *symmetric* (i.e., *homogeneous* and *self-dual*) cone [1, 25, 26]. The primal–dual scaling resulting from the theory of self-scaled barriers is known as the *Nesterov–Todd scaling*, and is the scaling used in several popular software packages, including SeDuMi [30], SDPT3 [33], and MOSEK [2].

Since Nesterov and Todd’s ground-breaking work on self-scaled barriers for symmetric cones, there has been substantial effort to extend some aspects of their primal–dual algorithms to nonsymmetric cones [3–6, 13–16, 23, 28, 29, 35, 36]. While not all nice properties of self-scaled barriers can be extended beyond symmetric cones (see [34, Theorem 4.2], [21, Lemma 6.4]), some of the critical, desired properties of primal–dual scalings induced by self-scaled barriers were extended to all logarithmically homogeneous self-concordant barriers (LHSCBs) and all convex cones [36]. In [36], a complexity measure of these primal–dual scalings is defined, which yields upper bounds on the iteration complexity of a class of interior-point algorithms utilizing the primal–dual scalings. In this paper, this complexity measure (defined below in Section 2.4) will be denoted by ξ_F , where F is a ϑ -logarithmically homogeneous self-concordant barrier (ϑ -LHSCB) for a convex cone K [18]. The complexity measure ξ_F is based on generalized eigenvalues of primal and dual Hessians relative to proximity of the arguments of the Hessians to the central path. The complexity measure ξ_F also admits a geometric interpretation in terms of Dikin ellipsoids (defined in Section 2.2). Locally, for a fixed pair of primal–dual interior-points (x, s) , ξ_F is related to the smallest blow-up factor for

the Dikin ellipsoid at x so that, it contains the dual of the Dikin ellipsoid at s when centered at x (also see the detailed explanation in Section 3.4 after equation (33)). The central role of ξ_F in the complexity analysis from [36] can be summarized as follows.

- In [36, Section 5], primal–dual interior-point algorithms for conic linear programming are described that achieve an

$$O(1)\xi_F\vartheta^{1/2}\ln(1/\epsilon) \quad (2)$$

iteration bound¹ where $O(1)$ denotes an absolute constant and F is the barrier used in the algorithm.

- It is known that $\xi_F \leq 9\vartheta(\vartheta - 1)$ for any ϑ -LHSCB F [22]. Combined with the iteration complexity bound (2), this gives an iteration bound

$$O(1)\vartheta^{5/2}\ln(1/\epsilon).$$

- If we consider a class of conic problems (P) with different cones K , each with a corresponding barrier F , and ξ_F is bounded by an absolute constant for all these barriers, then the iteration complexity for solving any instance in that class of conic problems is

$$O(\vartheta^{1/2}\ln(1/\epsilon)).$$

In particular, when $\xi_F \leq 4/3$, then $20\vartheta^{1/2}\ln(1/\epsilon)$ iterations suffice (the constant 20 can be improved).

The paper [36] also describes the properties of primal–dual scalings that are needed for these complexity bounds to apply. At each iteration of these algorithms, a primal–dual scaling can be selected from a convex set $\mathcal{T}(x^{(k)}, s^{(k)}; \hat{\xi})$ where $\hat{\xi} \geq \xi_F$ is a constant algorithm parameter. The set $\mathcal{T}(x^{(k)}, s^{(k)}; \hat{\xi})$ of acceptable scalings is defined by two systems of linear equality constraints and two matrix inequalities (see definition (16)).

This paper contains several new results on the complexity measure ξ_F and the associated sets of primal–dual scalings $\mathcal{T}(x, s; \hat{\xi})$.

- It is known that for self-scaled barriers of symmetric cones, $\xi_F \leq 4/3$, and that the Nesterov–Todd scaling is an element of $\mathcal{T}(x, s; 4/3)$ [36, Theorem 6.1]. In Section 3 we study ξ_F for LHSCBs with negative curvature, i.e., LHSCB barriers F with the additional property that $\langle F'(x), y \rangle$ is a concave function of x for any fixed $y \in K$. The class of convex cones which admit LHSCBs with negative curvature is much larger than the symmetric cones. For example, any barrier $F(x) := G(B(x))$ for a cone $K = \{x : B(x) \in C\}$, where B is a linear function, C is a symmetric cone, and G a self-scaled barrier for C , is an LHSCB with negative curvature, but not necessarily self-scaled. We show that the bound $\xi_F \leq 4/3$ holds for the family of LHSCBs with negative curvature. We further prove that the primal–dual integral scaling from [14] is an element of $\mathcal{T}(x, s; 4/3)$. An immediate consequence of this result is that the primal–dual potential reduction algorithm from [36], when implemented using the integral primal–dual scalings [14], has iteration complexity matching the current best bounds for conic optimization problems using cones with negative curvature barriers. This result impacts other primal–dual algorithms, e.g., the predictor–corrector algorithm analyzed in [14]. For negative curvature LHSCBs, our results imply that in some

¹Here, $\epsilon \in (0, 1)$, is a user-defined desired accuracy; the algorithms are required to generate a pair of primal–dual feasible solutions whose duality gap is at most ϵ times the original duality gap of the starting feasible primal–dual pair.

algorithms, during some iterations, we may take significantly larger predictor steps and still maintain $O(\vartheta^{1/2} \ln(1/\epsilon))$ iteration complexity bounds.

- In Section 4 we show that for optimal ϑ -self-scaled barriers F with $\vartheta \geq 2$,

$$\xi_F = \frac{(\tau_\vartheta + 1)^2}{\tau_\vartheta(\tau_\vartheta + 2)}, \quad \text{where } \tau_\vartheta := \sqrt{\frac{\vartheta}{\vartheta - 1}},$$

and that both the Nesterov–Todd scaling and the integral scaling from [14] are in $\mathcal{T}(x, s; \xi_F)$. The limit of ξ_F for $\vartheta \rightarrow +\infty$ is $4/3$, so the $4/3$ upper bound is asymptotically tight (see Figure 1).

- In the most general setting, with K any regular cone and F any ϑ -LHSCB, Øbro [22] has proved that $\xi_F \leq 9\vartheta(\vartheta - 1)$ (assuming $\vartheta \geq 2$). An improved upper bound of $\xi_F \leq 4\vartheta^2$ follows from the results in [21]. In Section 5, we improve these upper bounds, for a relaxation of ξ_F (defined in (3.4)), to $\check{\xi}_F \leq 2\vartheta$ and provide a localized analysis proving that this complexity measure stays bounded above by 4 outside a neighborhood of the central path. We also include numerical experiments which provide insights into the conditions which characterize good primal–dual scalings, and properties of pairs of primal and dual interior points where finding a good scaling is the most difficult.

Section 6 contains some concluding remarks and future research directions.

2. SELF-CONCORDANT BARRIERS AND PRIMAL–DUAL SCALINGS

Throughout the paper we assume K is a *regular* cone in \mathbb{R}^n and K^* is the dual cone defined in (1). We occasionally use the generalized inequality notation $x \succeq_K 0$ and $u \succeq_{K^*} 0$ as an alternative for $x \in K$ and $u \in K^*$. Without subscript, the inequality $A \preceq B$, where A and B are symmetric matrices, means that $B - A$ is positive semidefinite.

In this section we review some properties of logarithmically homogeneous self-concordant barriers, and the basic definitions and results on primal–dual scalings from [14, 36].

2.1. Minkowski gauge and norm. The *Minkowski gauge* for the cone K is the function that assigns to $x \in \text{int}(K)$ and $h \in \mathbb{R}^n$ the value

$$\sigma_x(h) := \inf \{ \beta \geq 0 : \beta x - h \in K \}. \quad (3)$$

The function $\sigma_x(\cdot)$ is convex, nonnegative, and positively homogeneous. If $-h \in K$, then $\sigma_x(h) = 0$. If $-h \notin K$, then $\sigma_x(h) > 0$ and $1/\sigma_x(h)$ is the step size from x to the boundary of K in the direction $-h$. We also note the identity

$$1 + \sigma_y(x - y) = \frac{1}{1 - \sigma_x(x - y)} \quad \text{for all } x, y \in \text{int}(K). \quad (4)$$

At every point $x \in \text{int}(K)$, a local *Minkowski norm* is defined as $|h|_x := \max \{ \sigma_x(h), \sigma_x(-h) \}$. In this paper, $\sigma_x(\cdot)$ and $|\cdot|_x$ always refer to the primal cone K . Therefore, no special notation is needed to distinguish these functions from the Minkowski gauge and norm associated with the dual cone K^* .

2.2. Logarithmically homogeneous self-concordant barriers. A ϑ -logarithmically homogeneous barrier for K is a closed convex function $F \in C^3$ (thrice continuously differentiable), with domain $\text{dom } F = \text{int}(K)$, which satisfies

$$F(tx) = F(x) - \vartheta \ln(t) \quad \text{for all } x \in \text{int}(K) \text{ and all } t > 0. \quad (5)$$

Such a barrier is called *self-concordant* if

$$F'''(x; h) \leq 2\|h\|_x F''(x) \quad \text{for all } x \in \text{int}(K) \text{ and all } h \in \mathbb{R}^n, \quad (6)$$

where $F''(x)$ is the Hessian at x , $F'''(x)$ the third derivative, and

$$\|h\|_x := \sqrt{\langle F''(x)h, h \rangle}. \quad (7)$$

On the left-hand side of (6), $F'''(x; h)$ is the directional third derivative of F at x , in the direction h ,

$$F'''(x; h) := \left. \frac{d}{d\alpha} F''(x + \alpha h) \right|_{\alpha=0}.$$

In later sections, we will refer to the following properties of ϑ -logarithmically homogeneous self-concordant barriers (ϑ -LHSCBs) [17, 18]. For a more detailed exposure to analysis of interior-point algorithms based on general self-concordant barriers, see [17, 18, 24].

- Logarithmic homogeneity (5) implies the identities

$$F'(tx) = \frac{1}{t} F'(x), \quad F''(tx) = \frac{1}{t^2} F''(x) \quad (8)$$

for all $x \in \text{int}(K)$ and $t > 0$, and

$$\langle F'(x), x \rangle = -\vartheta, \quad F''(x)x = -F'(x), \quad F'''(x; x) = -2F''(x) \quad (9)$$

for all $x \in \text{int}(K)$.

- The negative gradient at $x \in \text{int}(K)$ is in the interior of K^* : $-F'(x) \in \text{int}(K^*)$ for all $x \in \text{int}(K)$. Moreover, $-F' : \text{int}(K) \rightarrow \text{int}(K^*)$ is a bijection (see, for instance [34, Proposition 5.1]).
- The Hessian $F''(x)$ is positive definite for all $x \in \text{int}(K)$. Therefore the function $\|\cdot\|_x$ defined in (7) is a norm.
- The *Dikin ellipsoid* centered at x and with radius one, is contained in K :

$$E_{x,1} \subseteq K,$$

where $E_{x,r} := \{y \in \mathbb{R}^n : \|y - x\|_x \leq r\}$ is called the Dikin ellipsoid with center x and radius r . This property can also be expressed as

$$\sigma_x(h) \leq \|h\|_x \quad \text{for all } x \in \text{int}(K) \text{ and } h \in \mathbb{R}^n. \quad (10)$$

Applying this to $-h$, we also have $\sigma_x(-h) \leq \|h\|_x$ and therefore $|h|_x \leq \|h\|_x$.

- The variation of the Hessian on $\text{int}(K)$ is limited by the inequalities

$$(1 - \|y - x\|_x)^2 F''(x) \leq F''(y) \leq \frac{1}{(1 - \|y - x\|_x)^2} F''(x).$$

These matrix inequalities hold for all $x, y \in \text{int}(K)$ with $\|y - x\|_x < 1$.

The *dual barrier* associated with F is defined as

$$F_*(s) = \sup_{x \in \text{int}(K)} \{-\langle s, x \rangle - F(x)\}.$$

If F is a ϑ -LHSCB for K , then F_* is a ϑ -LHSCB for K^* . The dual barrier of the dual barrier F_* is equal to the original barrier F . The gradients and Hessians of F and F_* are related by the identities

$$F'_*(-F'(x)) = -x, \quad F'_*(-F'_*(s)) = -s, \quad (11)$$

and

$$F''_*(-F'(x)) = F''(x)^{-1}, \quad F''_*(-F'_*(s)) = F''_*(s)^{-1}. \quad (12)$$

We often use the notation

$$\tilde{s} := -F'(x), \quad \tilde{x} := -F'_*(s), \quad \mu := \frac{\langle s, x \rangle}{\vartheta}, \quad \tilde{\mu} := \frac{\langle \tilde{x}, \tilde{s} \rangle}{\vartheta} = \frac{\langle F'(x), F'_*(s) \rangle}{\vartheta}.$$

The points \tilde{s}, \tilde{x} are called the *shadows* of x and s , respectively. The notation $\tilde{s}, \tilde{x}, \mu, \tilde{\mu}$ is used when it is clear from the context what the corresponding points x and s are. Otherwise, we add s and x as explicit arguments of functions $\mu(x, s)$ and $\tilde{\mu}(x, s)$ defined as

$$\mu(x, s) := \frac{\langle s, x \rangle}{\vartheta}, \quad \tilde{\mu}(x, s) := \frac{\langle F'(x), F'_*(s) \rangle}{\vartheta}.$$

2.3. Central points and proximity measures. Points $x \in \text{int}(K)$ and $s \in \text{int}(K^*)$ form a *central pair* if s is a multiple of $-F'(x)$. Using (8), we see that the multiple is given by the positive quantity μ defined above. Thus, x, s form a central pair if and only if $s = -\mu F'(x) = \mu \tilde{s}$. From (11) and logarithmic homogeneity, the following four statements are equivalent (the last one is proved in Lemma 2.1):

$$x = \mu \tilde{x}, \quad \tilde{s} = \tilde{\mu} s, \quad \tilde{x} = \tilde{\mu} x, \quad \mu \tilde{\mu} = 1.$$

The motivation for this terminology is that if in addition x and s are feasible in their respective optimization problems, then (x, s) is a central pair if and only if (x, s) lies on the *primal–dual central path* (with the central path parameter set to $\mu(x, s)$).

Proximity measures that measure the deviation from centrality appear throughout the literature on interior-point methods. In this paper, the *gradient proximity measure* $\gamma_G(x, s)$ and the *uniform proximity measure* $\gamma_\infty(x, s)$, which are defined as

$$\gamma_G(x, s) := \vartheta(\mu \tilde{\mu} - 1), \quad \gamma_\infty(x, s) := \sigma_x(\mu \tilde{x}) - 1 \quad (13)$$

will be important. The suitability of γ_G and γ_∞ as proximity measures is stated in the following lemma.

Lemma 2.1. (Nesterov and Todd [20, pp. 343–344], [36, Lemma 4.1]) *If F is a ϑ -LHSCB for the regular cone K , then*

$$\vartheta \gamma_\infty(x, s) \geq \gamma_G(x, s) \geq 0, \quad \forall x \in \text{int}(K), \quad \forall s \in \text{int}(K^*).$$

Moreover, $\gamma_\infty(x, s) = \gamma_G(x, s) = 0$ if and only if x, s are a central pair.

Proof. Let F and K be as described in the assumptions. Let $x \in \text{int}(K)$ and $s \in \text{int}(K^*)$. Then,

$$\gamma_G(x, s) = \vartheta(\mu \tilde{\mu} - 1) = \langle F'(\mu \tilde{x}) - F'(x), \mu \tilde{x} - x \rangle \geq 0,$$

with equality only if $x = \mu\tilde{x}$. The second equality follows from

$$\langle F'(\mu\tilde{x}), \mu\tilde{x} \rangle = \langle F'(x), x \rangle = \langle F'(\mu\tilde{x}), x \rangle = -\vartheta, \quad \langle -F'(x), \tilde{x} \rangle = \vartheta\tilde{\mu}.$$

The inequality follows from the gradient monotonicity property of continuously differentiable convex functions (applied to F). Since F is strictly convex, equality holds above if and only if $x = \mu\tilde{x}$.

Since $\sigma_x(\mu\tilde{x}) = \mu\sigma_x(\tilde{x})$ ($\mu > 0$ and σ_x is positively homogeneous), the inequality $\vartheta\gamma_\infty(x, s) \geq \gamma_G(x, s)$ is equivalent to

$$\sigma_x(\tilde{x}) \geq \tilde{\mu}. \quad (14)$$

To show (14), we note that, by definition of $\sigma_x(\tilde{x})$, the point $\sigma_x(\tilde{x})x - \tilde{x} \in K$. Therefore, the inner product with $\tilde{s} = -F'(x) \in K^*$ is nonnegative:

$$0 \leq \langle \tilde{s}, \sigma_x(\tilde{x})x - \tilde{x} \rangle = \sigma_x(\tilde{x})\langle \tilde{s}, x \rangle - \langle \tilde{s}, \tilde{x} \rangle = \vartheta(\sigma_x(\tilde{x}) - \tilde{\mu}).$$

The last equation above follows from (9). If x, s are a central pair, then $x = \mu\tilde{x}$ and $\sigma_x(\mu\tilde{x}) = 1$, and equality holds throughout. Conversely, if the equality holds above, then, since $\tilde{s} \in \text{int}(K^*)$ and $\sigma_x(\tilde{x})x - \tilde{x} \in K$, we must have $\sigma_x(\tilde{x})x = \tilde{x}$. This implies $\tilde{\mu}x = \sigma_x(\tilde{x})x = \tilde{x}$ as desired. \square

For future reference, we add that the uniform proximity measure can also be written as

$$\gamma_\infty(x, s) = \sigma_x(\mu\tilde{x} - x) = \frac{\sigma_{\mu\tilde{x}}(\mu\tilde{x} - x)}{1 - \sigma_{\mu\tilde{x}}(\mu\tilde{x} - x)}. \quad (15)$$

The first equality follows from

$$\sigma_x(\mu\tilde{x} - x) = \inf \{ \beta \geq 0 : (\beta + 1)x - \mu\tilde{x} \in K \} = \sigma_x(\mu\tilde{x}) - 1,$$

since $\sigma_x(\mu\tilde{x}) \geq 1$ as shown in Lemma 2.1. The second equality in (15) follows from (4).

2.4. Primal–dual scalings. In this section we review some definitions and results from [14, 36]. For each pair $x \in \text{int}(K)$, $s \in \text{int}(K^*)$, a set of local primal–dual scalings is defined as

$$\mathcal{T}(x, s; \xi) := \left\{ T \in \mathbb{S}_{++}^n : Tx = s, T\tilde{x} = \tilde{s}, \frac{1}{\xi\delta_F(x, s)}F''(x) \leq T \leq \xi\delta_F(x, s)F''_*(s)^{-1} \right\}, \quad (16)$$

where ξ is a parameter and

$$\delta_F(x, s) := \frac{\gamma_G(x, s) + 1}{\mu} = \frac{\vartheta(\mu\tilde{\mu} - 1) + 1}{\mu} = \langle F'(x), F'_*(s) \rangle + \frac{\vartheta(\vartheta - 1)}{\langle s, x \rangle}. \quad (17)$$

This definition of \mathcal{T} corresponds to the set \mathcal{T}_2 from these earlier papers, where the subscript 2 was added to highlight the usage of second-order information on the barrier functions F and F_* .

The smallest value of ξ for which the set $\mathcal{T}(x, s; \xi)$ is nonempty for every pair $x \in \text{int}(K)$ and $s \in \text{int}(K^*)$ is denoted by ξ_F :

$$\xi_F := \inf \{ \xi : \mathcal{T}(x, s; \xi) \neq \emptyset, \forall (x, s) \in \text{int}(K) \oplus \text{int}(K^*) \}.$$

The importance of these definitions lies in the complexity analysis in [36]. If ξ_F is bounded above by an absolute constant, then the second-order algorithms in [36] and many other related algorithms based on primal–dual scalings are guaranteed to generate an ϵ -optimal solution in $O(\vartheta^{1/2} \ln(1/\epsilon))$ iterations. One of the key results in the theory of self-scaled barriers is the following.

Theorem 2.2. (Nesterov and Todd [19], see Theorem 6.1 in [36]) For every symmetric cone K and for every ϑ -self-scaled barrier F for K , we have

$$\xi_F \leq \frac{4}{3}.$$

Moreover, the Nesterov–Todd scaling is in $\mathcal{T}(x, s; 4/3)$ for every pair $x, s \in \text{int}(K)$.

A unique property of the Nesterov–Todd scaling is that it has the form $T = F''(w)$ for some (unique) point $w \in \text{int}(K)$. For non-symmetric cones, no scaling of the form $T = F''(w)$ exists that satisfies the two requirements

$$Tx = s, \quad T\tilde{x} = \tilde{s} \quad (18)$$

(see [14, section 6]). Motivated by this fact, the papers [14, 36] describe several methods to construct scalings that satisfy these conditions but are not of the form $T = F''(w)$. For our purposes the *integral scaling* from [14, section 3] will be the most relevant. The integral scaling is defined as

$$T := \mu \int_0^1 F''((1 - \alpha)x + \alpha(\mu\tilde{x})) d\alpha. \quad (19)$$

For a proof that this integral satisfies (18), see [14, Theorem 3.1].

3. BARRIERS WITH NEGATIVE CURVATURE

Theorem 2.2 states that $\xi_F \leq 4/3$ for self-scaled barriers F and that the Nesterov–Todd scaling is in $\mathcal{T}(x, s; 4/3)$ for all $x, s \in \text{int}(K)$. In this section we extend this result to self-concordant barriers with negative curvature. These barriers form a special class of self-concordant barrier functions that strictly includes the self-scaled barriers and are defined for convex cones that are strictly more general than homogeneous cones. In Sections 3.1–3.3, we define negative curvature barriers and discuss the most important properties. Section 3.4 contains the main result on the complexity measure and primal–dual metrics.

3.1. Negative curvature.

Definition 3.1. A logarithmically homogeneous barrier F for a regular convex cone K has negative curvature if for every $u \in K$, the function

$$f_u(x) := \langle F'(x), u \rangle, \quad (20)$$

with $\text{dom } f_u = \text{int}(K)$, is concave in x .

Several equivalent definitions follow from the various characterizations of concavity of the function f_u . For example, Jensen’s inequality

$$f_u(\alpha x + (1 - \alpha)y) \geq \alpha f_u(x) + (1 - \alpha)f_u(y) \quad \forall u \in K, \forall x, y \in \text{int } K, \forall \alpha \in [0, 1],$$

is equivalent to the vector inequality

$$F'(\alpha x + (1 - \alpha)y) \succeq_{K^*} \alpha F'(x) + (1 - \alpha)F'(y) \quad \forall x, y \in \text{int } K, \forall \alpha \in [0, 1]. \quad (21)$$

Hence negative curvature means that the gradient of F is K^* -concave.

Negative curvature barriers were studied by Güler in [10] and by Nesterov and Tunçel in [21]. They include the self-scaled barriers for symmetric cones [19, Lemma 3.1], but are much more general.

For example, composition with a linear mapping preserves negative curvature, but in general not self-scaledness. Therefore, the barrier

$$F(x) := -\ln \det(x_1 A_1 + x_2 A_2 + \cdots + x_n A_n),$$

where $A_1, \dots, A_n \in \mathbb{S}^m$ are linearly independent, is an m -logarithmically homogeneous barrier with negative curvature for the regular cone $K := \{x \in \mathbb{R}^n : x_1 A_1 + x_2 A_2 + \cdots + x_n A_n \succeq 0\}$.

3.2. Bounds on derivatives and function values. From the values and derivatives of a negative-curvature barrier F at a point $x \in \text{int}(K)$, one obtains bounds on the values and derivatives at other points in the interior of K . For the second derivatives, this property is referred to as the *long-step Hessian estimation property* in [14]. The inequalities listed in the next proposition are known to hold for self-scaled barriers for symmetric cones [19, 20], but are derived here under the weaker assumptions of logarithmic homogeneity and negative curvature. See, also [10, Section 7].

Proposition 3.2. *Let F be a logarithmically homogeneous barrier for the regular cone K . If F has negative curvature, then the following properties hold.*

- For all $x \in \text{int}(K)$ and all h ,

$$-2\sigma_x(h)F''(x) \leq F'''(x; h) \leq 2\sigma_x(-h)F''(x). \quad (22)$$

- For all $x, y \in \text{int}(K)$,

$$\frac{1}{(1 + \sigma_x(y - x))^2} F''(x) \leq F''(y) \leq \frac{1}{(1 - \sigma_x(x - y))^2} F''(x). \quad (23)$$

- For all $x, y \in \text{int}(K)$,

$$\frac{\|y - x\|_x^2}{1 + \sigma_x(y - x)} \leq \langle F'(y) - F'(x), y - x \rangle \leq \frac{\|y - x\|_x^2}{1 - \sigma_x(x - y)}. \quad (24)$$

Note that $0 \leq \sigma_x(x - y) < 1$ for all $x, y \in \text{int}(K)$, so the bounds in (23) and (24) are well defined.

Proof. We start with the second inequality in (22). Suppose $x \in \text{int}(K)$. By definition of $\sigma_x(-h)$, the vector $u = \sigma_x(-h)x + h$ is in K . Since F has negative curvature, the function $f_u = \langle F'(\cdot), u \rangle$ is concave. The Hessian $f_u''(x) = F'''(x; u)$ at x satisfies

$$0 \geq F'''(x; u) = \sigma_x(-h)F'''(x; x) + F'''(x; h) = -2\sigma_x(-h)F''(x) + F'''(x; h).$$

The last step uses $F'''(x; x) = -2F''(x)$, which follows from logarithmic homogeneity (see (9)). The first inequality in (22) is the second inequality applied to $-h$, since $F'''(x; -h) = -F'''(x; h)$.

To prove (23), we define $h = x - y$ and $g(\alpha) = \langle F''(x - \alpha h)v, v \rangle$ for fixed nonzero v . From (22),

$$\frac{-2\sigma_x(-h)}{1 + \alpha\sigma_x(-h)} = -2\sigma_{x-\alpha h}(-h) \leq \frac{g'(\alpha)}{g(\alpha)} \leq 2\sigma_{x-\alpha h}(h) = \frac{2\sigma_x(h)}{1 - \alpha\sigma_x(h)}.$$

The right-hand side holds if $\alpha\sigma_x(h) < 1$. The left-hand side holds for all $\alpha \geq 0$. Integration gives

$$-2 \ln(1 + \alpha\sigma_x(-h)) \leq \ln \frac{g(\alpha)}{g(0)} \leq -2 \ln(1 - \alpha\sigma_x(h))$$

and therefore

$$\frac{g(0)}{(1 + \alpha\sigma_x(-h))^2} \leq g(\alpha) \leq \frac{g(0)}{(1 - \alpha\sigma_x(h))^2}.$$

For $\alpha = 1$, this is (23).

Next, to show (24) we use the expression

$$-\langle F'(y) - F'(x), h \rangle = \int_0^1 \langle F''(x - \alpha h)h, h \rangle d\alpha$$

and bound the right-hand side by integrating (23) (and using $\sigma_x(\alpha v) = \alpha \sigma_x(v)$ for nonnegative α):

$$\|h\|_x^2 \int_0^1 \frac{1}{(1 + \alpha \sigma_x(-h))^2} d\alpha \leq -\langle F'(y) - F'(x), h \rangle \leq \|h\|_x^2 \int_0^1 \frac{1}{(1 - \alpha \sigma_x(h))^2} d\alpha.$$

The integrals are

$$\int_0^1 \frac{1}{(1 + \alpha \sigma_x(-h))^2} d\alpha = \frac{1}{1 + \sigma_x(-h)}, \quad \int_0^1 \frac{1}{(1 - \alpha \sigma_x(h))^2} d\alpha = \frac{1}{1 - \sigma_x(h)}.$$

□

We mention two more results which provide bounds on Hessians of negative-curvature barriers.

Proposition 3.3. (See also [10, Corollary 7.2]) *Let F be a logarithmically homogeneous barrier for the regular cone K . If F has negative curvature, then for all $x, y \in \text{int}(K)$,*

$$F''(y) \leq \sigma_y(x)^2 F''(x). \quad (25)$$

In particular, if $y - x \in K$, then $\sigma_y(x) \leq 1$ and therefore $F''(y) \leq F''(x)$.

Proof. Define $h = x - \sigma_y(x)y$. Since $-h \in K$ (by definition of $\sigma_y(x)$), we have $\sigma_x(h) = 0$. From the right-hand inequality of (23),

$$\frac{1}{\sigma_y(x)^2} F''(y) = F''(\sigma_y(x)y) \leq \frac{1}{(1 - \sigma_x(h))^2} F''(x) = F''(x).$$

□

The inequality (25) gives a bound on the generalized eigenvalues of the matrix pair $F''(y), F''(x)$:

$$\lambda_{\max}(F''(x)^{-1} F''(y)) \leq \sigma_y(x)^2. \quad (26)$$

Later, we will see that for self-scaled barriers equality holds; see Lemma 4.2.

Proposition 3.4. *Let F be a logarithmically homogeneous barrier for the regular cone K . For $x, y \in \text{int}(K)$, define*

$$G := \int_0^1 F''((1 - \alpha)x + \alpha y) d\alpha.$$

If F has negative curvature, then

$$\frac{1}{1 + \sigma_x(y - x)} F''(x) \leq G \leq \frac{1}{1 - \sigma_x(x - y)} F''(x) \quad (27)$$

and

$$(1 - \sigma_x(x - y)) F''(y) \leq G \leq (1 + \sigma_x(y - x)) F''(y). \quad (28)$$

Proof. We integrate the bounds in (23). Define $h = x - y$. For the upper bound,

$$G \leq \left(\int_0^1 \frac{1}{(1 - \alpha \sigma_x(h))^2} d\alpha \right) F''(x) = \frac{1}{1 - \sigma_x(h)} F''(x).$$

For the lower bound,

$$G \geq \left(\int_0^1 \frac{1}{(1 + \alpha \sigma_x(-h))^2} d\alpha \right) F''(x) = \frac{1}{1 + \sigma_x(-h)} F''(x).$$

This proves (27). Switching x and y in these inequalities gives

$$\frac{1}{1 + \sigma_y(x - y)} F''(y) \leq G \leq \frac{1}{1 - \sigma_y(y - x)} F''(y).$$

The inequalities (28) follow from the identity (4). \square

3.3. Proximity measures. The next proposition, which gives an inequality between the gradient and uniform proximity measures, was proved for self-scaled barriers in [20, Theorem 4.2].

Proposition 3.5. *Let F be a ϑ -LHSCB with negative curvature. Then for all $x \in \text{int}(K)$, $s \in \text{int}(K^*)$,*

$$\gamma_G(x, s) \geq \frac{\gamma_\infty(x, s)^2}{1 + \gamma_\infty(x, s)}. \quad (29)$$

Proof. From the first inequality in (24) applied to $y = \mu\tilde{x}$, we find that

$$\gamma_G(x, s) = \langle F'(\mu\tilde{x}) - F'(x), \mu\tilde{x} - x \rangle \geq \frac{\|\mu\tilde{x} - x\|_x^2}{\sigma_x(\mu\tilde{x})} = \frac{\|\mu\tilde{x} - x\|_x^2}{1 + \gamma_\infty(x, s)}. \quad (30)$$

Self-concordance of F further implies that $\|h\|_x \geq |h|_x$ for all $x \in \text{int}(K)$ and all h . Therefore

$$\|\mu\tilde{x} - x\|_x \geq |\mu\tilde{x} - x|_x \geq \sigma_x(\mu\tilde{x} - x) = \gamma_\infty(x, s), \quad (31)$$

by the first identity in (15). Combining (30) and (31) gives (29). \square

Simpler lower bounds on γ_G are

$$\gamma_G(x, s) \geq \frac{3\gamma_\infty(x, s) - 1}{4}, \quad \gamma_\infty(x, s) \leq \frac{4\gamma_G(x, s) + 1}{3}. \quad (32)$$

The first one follows from $x^2/(1+x) \geq (3x-1)/4$, the linear approximation of the convex function $x^2/(1+x)$ at $x = 1$.

3.4. Bounds on the complexity measures for primal–dual scalings. We now return to the complexity parameter ξ_F . To simplify the analysis and improve our understanding of ξ_F , it will be useful to relax the set (16) by omitting the equality constraints $Tx = s$ and $T\tilde{x} = \tilde{s}$. Define

$$\check{\mathcal{T}}(x, s; \xi) := \left\{ T \in \mathbb{S}_{++}^n : \frac{1}{\xi \delta_F(x, s)} F''(x) \leq T \leq \xi \delta_F(x, s) F''(x) \right\}$$

and

$$\check{\xi}_F := \inf \left\{ \xi : \check{\mathcal{T}}(x, s; \xi) \neq \emptyset, \forall x \in \text{int}(K), s \in \text{int}(K^*) \right\}. \quad (33)$$

The complexity measure $\check{\xi}_F$ admits an intriguing geometric interpretation. For every pair of primal–dual interior points (x, s) , consider the smallest blow-up factor for the Dikin ellipsoid at x with

radius $\delta_F^2(x, s)$ so that it contains the dual of the Dikin ellipsoid (for F_*) with radius one at s when that dual ellipsoid is centered at x . Then $\check{\xi}_F$ is the supremum of all of these smallest blow-up factors over all primal–dual pairs of interior points (x, s) (i.e., the smallest blow-up factor that guarantees the above ellipsoid containment property for all primal–dual pairs (x, s)).

Clearly, $\mathcal{T}(x, s; \xi) \subseteq \check{\mathcal{T}}(x, s; \xi)$ and $\xi_F \geq \check{\xi}_F$. The set $\check{\mathcal{T}}(x, s; \xi)$ is nonempty if and only if

$$F''(x) \preceq (\xi \delta_F(x, s))^2 F''_*(s)^{-1},$$

i.e., $\xi \delta_F(x, s)$ is greater than or equal to the square root of the largest eigenvalue of the matrix product $F''_*(s)^{-1} F''(x)$. Therefore,

$$\check{\xi}_F = \sup_{x \in \text{int}(K), s \in \text{int}(K^*)} \left\{ \frac{\lambda_{\max}^{1/2}(F''(x) F''_*(s))}{\delta_F(x, s)} \right\} \leq \sup_{x \in \text{int}(K), s \in \text{int}(K^*)} \frac{\sigma_x(\tilde{x})}{\delta_F(x, s)}. \quad (34)$$

The inequality follows from (26).

Theorem 3.6. *Let F be a ϑ -LHSCB with negative curvature. Then $\check{\xi}_F \leq 4/3$.*

Proof. From (34),

$$\check{\xi}_F \leq \sup_{x \in \text{int}(K), s \in \text{int}(K^*)} \frac{\sigma_x(\tilde{x})}{\delta_F(x, s)} = \sup_{x \in \text{int}(K), s \in \text{int}(K^*)} \frac{\gamma_\infty(x, s) + 1}{\gamma_G(x, s) + 1} \leq 4/3.$$

The equality follows from the definitions of $\gamma_\infty(x, s)$ in (13) and of $\delta_F(x, s)$ in (17). For the second inequality we use the bound $\gamma_\infty(x, s) + 1 \leq 4(\gamma_G(x, s) + 1)/3$ from (32). \square

Theorem 3.7. *Let F be a ϑ -LHSCB with negative curvature. Then $\xi_F \leq 4/3$. Moreover, the integral scaling (19) is in $\mathcal{T}(x, s; 4/3)$.*

Proof. Let T be the integral scaling (19) for a primal–dual pair $x \in \text{int}(K)$, $s \in \text{int}(K^*)$. We verify that $T \in \mathcal{T}(x, s; 4/3)$. By Theorem 3.1 in [14], T satisfies the two systems of linear equations $Tx = s$ and $T\tilde{x} = \tilde{s}$. From the first inequality in (27) and the second inequality in (28), applied with $y = \mu\tilde{x}$,

$$\frac{\mu}{1 + \sigma_x(\mu\tilde{x} - x)} F''(x) \preceq T \preceq \frac{1 + \sigma_x(\mu\tilde{x} - x)}{\mu} F''(\tilde{x}). \quad (35)$$

Here,

$$\frac{1 + \sigma_x(\mu\tilde{x} - x)}{\mu} = \frac{\gamma_\infty(x, s) + 1}{\mu} \leq \frac{4(\gamma_G(x, s) + 1)}{3\mu} = \frac{4}{3} \delta_F(x, s).$$

The first equality follows from (15). The inequality is from (32). \square

4. SELF-SCALED BARRIERS FOR SYMMETRIC CONES

In this section we consider self-scaled barriers for symmetric cones. We derive the exact value of ξ_F as a function of the barrier parameter ϑ and show that both the Nesterov–Todd scaling and the integral scaling are in $\mathcal{T}(x, s; \xi_F)$. We will see that $\xi_F \rightarrow 4/3$ as $\vartheta \rightarrow \infty$, so the $4/3$ upper bound from Theorem 2.2 is asymptotically tight. The proofs of these results give insight into the worst-case pairs (x, s) , i.e., pairs with the property that $\mathcal{T}(x, s; \xi)$ is empty for $\xi < \xi_F$.

4.1. Self-scaled barriers. The main result of this section (Theorem 4.3) will use the following two lemmas, where the first one gathers results on self-scaled barriers from Nesterov and Todd [19, 20].

Lemma 4.1. *Let K be a symmetric cone and let F be a ϑ -self-scaled barrier for K . Then, we have the following properties.*

(1) *Let $x, w \in \text{int}(K)$ and $s := F''(w)x$. Then,*

$$F'(x) = F''(w)F'_*(s) \quad \text{and} \quad F''(x) = F''(w)F''_*(s)F''(w). \quad (36)$$

(2) *For every pair $x \in \text{int}(K)$, $s \in \text{int}(K^*)$ there exists a unique $w \in \text{int}(K)$ that satisfies $F''(w)x = s$. The scaling point w also satisfies $F''(w)\tilde{x} = \tilde{s}$.*

(3) *F has negative curvature.*

(4) *Let $w \in \text{int}(K)$ and $y, v \in \text{bd}(K)$ satisfy $\langle F''(w)y, v \rangle = 0$. Then,*

$$\langle F''(w + \alpha v + \beta y)v, v \rangle = \langle F''(w + \alpha v)v, v \rangle \quad \text{for all } \alpha, \beta \geq 0. \quad (37)$$

The matrix $F''(w)$ at the scaling point w in the second property is commonly referred to as the *Nesterov–Todd scaling* at x, s .

Proof. The gradient and Hessian scaling property was given in [19, equations (3.1) and (3.2)]. The existence and uniqueness of the scaling point is proved in [19, Theorem 3.2]. The negative curvature property is [19, Lemma 3.1]. The last property is given in [19, Theorem 5.1]. \square

The next lemma strengthens the result of [19, Corollary 4.1 (ii), (iii)].

Lemma 4.2. *Let K be a symmetric cone and let F be a ϑ -self-scaled barrier for K . Suppose $x, w \in \text{int}(K)$ and $s \in \text{int}(K^*)$ satisfy $F''(w)x = s$. Then we have the following properties, where q is any nonzero vector in $\text{bd}(K)$ that satisfies*

$$\langle F''(w)q, \sigma_x(w)x - w \rangle = 0.$$

(By definition of $\sigma_x(w)$ and $F''(w)K = K^*$ such a vector q exists.)

(1) *Relation between $\sigma_x(\tilde{x})$ and $\sigma_x(w)$:*

$$\sigma_x(\tilde{x}) = \sigma_x(w)^2, \quad \langle F''(w)q, \sigma_x(\tilde{x})x - \tilde{x} \rangle = 0.$$

(2) *Maximum generalized eigenvalue of Hessian pairs:*

$$\lambda_{\max}(F''(w)^{-1}F''(x)) = \lambda_{\max}(F''_*(s)F''(w)) = \lambda_{\max}^{1/2}(F''_*(s)F''(x)) = \sigma_x(\tilde{x}), \quad (38)$$

and q is a corresponding eigenvector,

$$F''(x)q = \sigma_x(\tilde{x})F''(w)q, \quad F''(w)q = \sigma_x(\tilde{x})F''(\tilde{x})q, \quad F''(x)q = \sigma_x(\tilde{x})^2F''(\tilde{x})q. \quad (39)$$

Proof. The first statement is a part of [20, Lemma 3.4] and its proof. The Hessian scaling property of self-scaled barriers (Lemma 4.1) implies that

$$F''(w)^{-1}F''(x) = F''_*(s)F''(w), \quad F''_*(s)F''(x) = (F''(w)^{-1}F''(x))^2 = (F''_*(s)F''(w))^2. \quad (40)$$

Since products of positive definite matrices have real, positive eigenvalues, the first two equalities in (38) follow. Next, we prove that $\lambda_{\max}(F''(w)^{-1}F''(x)) = \sigma_x(w)^2$. Since self-scaled barriers have negative curvature, it follows from (26) that

$$\lambda_{\max}(F''(w)^{-1}F''(x)) \leq \sigma_x(w)^2. \quad (41)$$

By definition of $\sigma_x(w)$, we have $y := \sigma_x(w)x - w \in \text{bd}(K)$, so there exists a nonzero $z \in \text{bd}(K^*)$ such that $\langle z, y \rangle = 0$. Let $q := F''(w)^{-1}z$. Then $y, q \in \text{bd}(K)$ and $\langle F''(w)q, y \rangle = 0$, and the fourth property in Lemma 4.1 (with $\alpha = 0, \beta = 1$) implies that

$$\frac{1}{\sigma_x(w)^2} \langle F''(x)q, q \rangle = \langle F''(\sigma_x(w)x)q, q \rangle = \langle F''(w + y)q, q \rangle = \langle F''(w)q, q \rangle.$$

Hence

$$\frac{\langle F''(x)q, q \rangle}{\langle F''(w)q, q \rangle} = \sigma_x(w)^2, \quad (42)$$

which shows that equality holds in (41) and that q is a generalized eigenvector of the matrix pair $F''(x), F''(w)$, i.e., the first equality in (39). The other two equalities follow from (40). \square

Lemma 4.2 gives a simplification of the expression for $\check{\xi}_F$ in (34). This is stated in the next theorem. The second equality in (43) should be compared with the inequality (34) for barriers with negative curvature.

Theorem 4.3. *Let K be a symmetric cone and F be a ϑ -self-scaled barrier for K . Then,*

$$\xi_F = \check{\xi}_F = \sup_{x \in \text{int}(K), s \in \text{int}(K^*)} \frac{\sigma_x(\tilde{x})}{\delta_F(x, s)} = \sup_{x, w \in \text{int}(K)} \frac{\sigma_x(w)^2}{\delta_F(x, F''(w)x)}. \quad (43)$$

Moreover, for every pair of interior points $x \in \text{int}(K)$, $s \in \text{int}(K^*)$, the Nesterov–Todd scaling and the integral scaling (19) at (x, s) are in $\mathcal{T}(x, s; \xi_F)$.

Proof. Let K be a symmetric cone and F be a ϑ -self-scaled barrier for K . The second and third equations in (43) follow by substituting $\sigma_x(\tilde{x})$ and $\sigma_x(w)^2$ for the root of the maximum eigenvalue in (34), using Lemma 4.2.

Next, we prove that $\xi_F = \check{\xi}_F$ and that the Nesterov–Todd scaling at (x, s) is in $\mathcal{T}(x, s; \xi_F)$. Since $\xi_F \geq \check{\xi}_F$, both claims are proved if we show that the Nesterov–Todd scaling is in $\mathcal{T}(x, s; \check{\xi}_F)$. Let $T = F''(w)$ be the Nesterov–Todd scaling at x, s . The equality constraints $Tx = s$ and $T\tilde{x} = \tilde{s}$ in the definition of $\mathcal{T}(x, s; \check{\xi}(T))$ follow from Lemma 4.1, part (2). The two matrix inequalities

$$\frac{1}{\check{\xi}_F \delta_F(x, s)} F''(x) \leq T \leq \check{\xi}_F \delta_F(x, s) F''_*(s)^{-1}, \quad (44)$$

for $T = F''(w)$ follow from Lemma 4.2 and the definition of $\check{\xi}_F$ in (34) (see also [19, Corollary 4.1]).

To see that the integral scaling (19) is also in $\mathcal{T}(x, s; \xi_F)$, we strengthen the result in Theorem 3.7. As noted in the proof of that theorem, the integral scaling satisfies $Tx = s$ and $T\tilde{x} = \tilde{s}$, and the inequalities (35). Since $\sigma_x(\mu\tilde{x} - x) = \mu\sigma_x(\tilde{x})$ (see (15)), the inequalities (35) can be written as

$$\frac{1}{\sigma_x(\tilde{x})} F''(x) \leq T \leq \sigma_x(\tilde{x}) F''(\tilde{x}).$$

By (43) we have $\sigma_x(\tilde{x}) \leq \check{\xi}_F \delta_F(x, s)$. Hence the inequalities (44) hold for the integral scaling T . \square

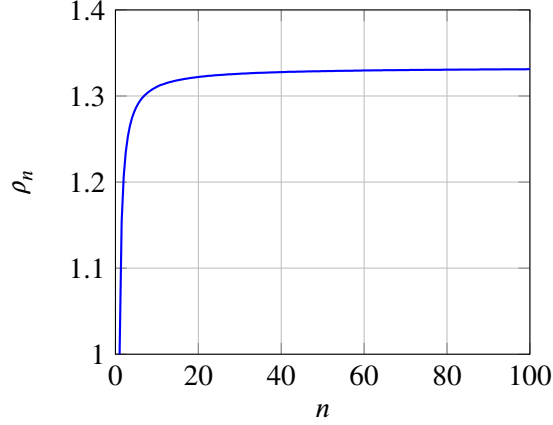


FIGURE 1. The function ρ_n defined in (45). The limit for $n \rightarrow \infty$ is $4/3$.

In the following sections we work out the exact value of ξ_F for commonly used self-scaled barriers. To simplify the notation, we define

$$\tau_n := \sqrt{\frac{n}{n-1}}, \quad \rho_n := \frac{(\tau_n + 1)^2}{\tau_n(\tau_n + 2)}, \quad (45)$$

for integers $n \geq 2$. Figure 1 shows ρ_n as a function of n .

4.2. Nonnegative orthant. We start with the nonnegative orthant ($K = K^* = \mathbb{R}_+^n$) and the logarithmic barrier function $F : \mathbb{R}^n \rightarrow \mathbb{R} \cup \{+\infty\}$ defined by

$$F(x) := \begin{cases} -\sum_{j=1}^n \ln x_j, & \text{if } x \in \mathbb{R}_{++}^n, \\ +\infty, & \text{otherwise.} \end{cases} \quad (46)$$

This is a self-scaled barrier with $\vartheta = n$. The dual barrier is

$$F_*(s) := \begin{cases} -\sum_{j=1}^n \ln s_j - n, & \text{if } s \in \mathbb{R}_{++}^n, \\ +\infty, & \text{otherwise.} \end{cases}$$

Theorem 4.4. *Let F be the barrier function (46), with $n \geq 2$. Then $\xi_F = \check{\xi}_F = \rho_n$. Moreover, for every pair $x, s \in \mathbb{R}_{++}^n$, the diagonal matrix T with diagonal entries $T_{ii} = s_i/x_i$ is in $\mathcal{T}(x, s; \xi_F)$.*

Proof. Let $x, s \in \mathbb{R}_{++}^n$. Then

$$\sigma_x(\tilde{x}) = \frac{1}{\min_i \{x_i s_i\}}, \quad \delta_F(x, s) = n\tilde{\mu} - \frac{n-1}{\mu} = \sum_{i=1}^n \frac{1}{x_i s_i} - \frac{n(n-1)}{\sum_i x_i s_i}$$

and therefore

$$\frac{1}{\check{\xi}_F} = \inf_{x, s \in \mathbb{R}_{++}^n} \left(\min_{i \in \{1, \dots, n\}} v_i \left(\sum_{j=1}^n \frac{1}{v_j} - \frac{n(n-1)}{\sum_j v_j} \right) \right), \quad (47)$$

where $v \in \mathbb{R}_{++}^n$ is the vector with components $v_i = x_i s_i$ for $i \in \{1, \dots, n\}$. (The vector v is the component-wise square of the usual v -space vector from the interior-point literature.) To solve

the minimization problem in this expression, we can assume, without loss of generality, that $v_n = \min_i v_i = 1$. Therefore, $1/\check{\xi}_F$ is the optimal value of the optimization problem

$$\begin{aligned} & \text{minimize} && 1 + \sum_{j=1}^{n-1} \frac{1}{v_j} - \frac{n-1}{\alpha} \\ & \text{subject to} && v_i \geq 1, \quad i \in \{1, 2, \dots, n-1\} \\ & && 1 + \sum_{i=1}^{n-1} v_i = n\alpha, \end{aligned} \tag{48}$$

with variables v_1, \dots, v_{n-1} and α . We solve the problem with the inequalities omitted and will find that they are inactive at the optimum. For fixed α , the problem is convex and the optimality conditions are

$$\frac{1}{v_i^2} = \lambda, \quad i \in \{1, \dots, n-1\}, \quad 1 + \sum_{i=1}^{n-1} v_i = n\alpha,$$

where λ is a Lagrange multiplier for the equality constraint. Hence, for given α , the variables v_1, \dots, v_{n-1} are equal at the optimum. From the equality constraint, $v_i = \tau_n^2(\alpha - 1) + 1$ for $i \in \{1, \dots, n-1\}$. Substitution in the objective function of (48) gives the optimal value as a function of α ,

$$f(\alpha) := 1 + \frac{n-1}{\tau_n^2(\alpha - 1) + 1} - \frac{n-1}{\alpha}.$$

This is minimized by $\alpha = 1 + 1/\tau_n$ and the optimal value is $f(1 + 1/\tau_n) = \rho_n$. We conclude that the optimal value and optimal solution of (48) are

$$\frac{1}{\check{\xi}_F} = \inf_{\alpha} f(\alpha) = \rho_n, \quad v = (\tau_n + 1, \dots, \tau_n + 1, 1). \tag{49}$$

The last statement in the theorem follows from Theorem 4.3 and the fact that the diagonal matrix with diagonal entries s_i/x_i is the Nesterov–Todd scaling for the barrier F . \square

The proof established that the value of $\check{\xi}_F$ is attained by pairs (x, s) with component-wise product v given by (49). For these worst-case pairs, $\mu = (\tau_n + 1)/\tau_n$. Other worst-case pairs are constructed by permuting and scaling the solution v in (49).

Corollary 4.5. *Let F be the barrier function (46), with $n \geq 2$. Then for every $s \in \mathbb{R}_{++}^n$, there is an $x \in \mathbb{R}_{++}^n$ which together with s attains $\check{\xi}_F$. In particular, for each $\mu > 0$, pick any $i \in \{1, 2, \dots, n\}$ and set*

$$x_j := \begin{cases} (\tau_n/(\tau_n + 1))\mu\tilde{x}_i, & \text{if } j = i; \\ \tau_n\mu\tilde{x}_j, & \text{otherwise,} \end{cases} \tag{50}$$

where $\tilde{x}_j = 1/s_j$ for $j \in \{1, 2, \dots, n\}$.

It can be verified that for all worst-case pairs described in the corollary,

$$\gamma_G(x, s) = \frac{1}{\tau_n + 1}, \quad \gamma_\infty(x, s) = \frac{1}{\tau_n}, \quad \|x - \mu\tilde{x}\|_{\mu\tilde{x}} = \frac{\tau_n}{\tau_n + 1}.$$

Figure 2 illustrates the corollary in dimension $n = 3$. In the figure, the nonnegative orthant in \mathbb{R}^3 is intersected with the plane $\{x \in \mathbb{R}^n : \langle s, x \rangle = n\mu\}$, for a given positive vector s and constant $\mu > 0$. The point $\mu\tilde{x}$ in the plane forms a central pair with s . The two elliptical curves show the

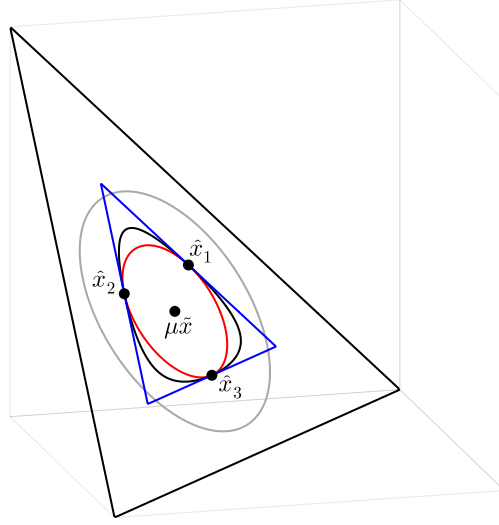


FIGURE 2. Nonnegative orthant of \mathbb{R}^n for $n = 3$ intersected with a hyperplane $\{x \in \mathbb{R}^n : \langle s, x \rangle = n\mu\}$ where s is a positive vector. The gray curve is the boundary of the unit Dikin ellipsoid centered at $\mu\tilde{x}$. The points $\hat{x}_1, \hat{x}_2, \hat{x}_3$ are the three points in the plane that attain $\check{\xi}_F$, as given by Corollary 4.5. They lie on the boundary of the Dikin ellipsoid with radius $\tau_n/(\tau_n + 1)$ (red curve). The black curve shows the boundary of the neighborhood $\gamma_G(x, s) \leq 1/(\tau_n + 1)$. The blue triangle is the boundary of the neighborhood $\gamma_\infty(x, s) \leq 1/\tau_n$.

boundaries of the Dikin ellipsoids $E_{\mu\tilde{x}, r} = \{x \in \mathbb{R}^n : \|x - \mu\tilde{x}\|_{\mu\tilde{x}} \leq r\}$ with radius $r = 1$ (gray curve) and $r = \tau_n/(\tau_n + 1)$ (red curve). The points $\hat{x}_1, \hat{x}_2, \hat{x}_3$ are the three points in the plane that attain $\check{\xi}_F$ together with s . The black curve is the contour line of $\gamma_G(x, s) = 1/(\tau_n + 1)$ and the blue curve is the contour line of $\gamma_\infty(x, s) = 1/\tau_n$.

4.3. Positive semidefinite cone. For the cone of symmetric positive semidefinite matrices $K = K^* = \mathbb{S}_{++}^m$, the barrier

$$F(x) := \begin{cases} -\ln \det(x), & \text{if } x \in \mathbb{S}_{++}^m; \\ +\infty, & \text{otherwise,} \end{cases} \quad (51)$$

and the corresponding dual barrier

$$F_*(s) := \begin{cases} -\ln \det(s) - m, & \text{if } s \in \mathbb{S}_{++}^m; \\ +\infty, & \text{otherwise,} \end{cases}$$

are self-scaled with $\vartheta = m$. Here, the dual cone and dual barrier are defined with respect to the trace inner product $\langle s, x \rangle = \text{Tr}(sx)$.

Theorem 4.6. *Let F be the barrier function (51), with $m \geq 2$. Then $\xi_F = \check{\xi}_F = \rho_m$. Moreover, the Nesterov–Todd scaling and the integral scaling at x, s are in $\mathcal{T}(x, s; \xi_F)$.*

Proof. Let $x, s \in \mathbb{S}_{++}^m$. Then

$$\sigma_x(\tilde{x}) = \lambda_{\min}(xs) \quad \delta_F(x, s) = \text{Tr}(x^{-1}s^{-1}) - \frac{m(m-1)}{\text{Tr}(xs)}.$$

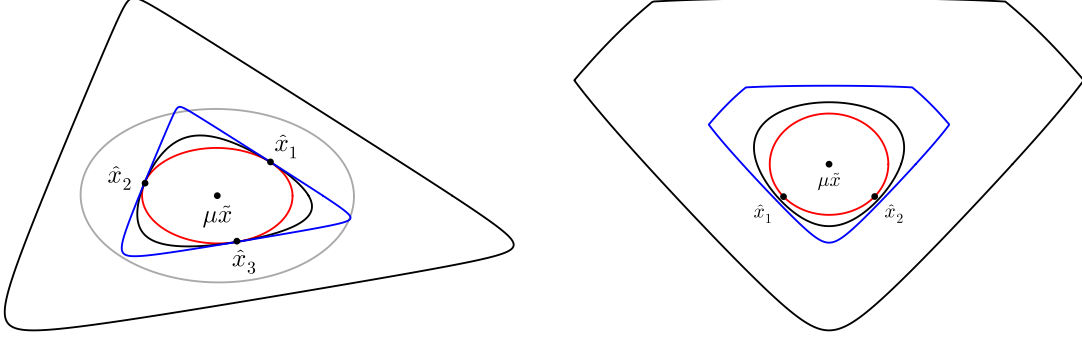


FIGURE 3. *Left.* The intersection of the three-dimensional positive semidefinite cone \mathbb{S}_+^2 and the hyperplane defined by $\langle x, s \rangle = 2\mu$ for a given s and μ . *Right.* Tridiagonal Toeplitz cone intersected with the hyperplane $\{x \in \mathbb{R}^3 : \langle x, s \rangle = \mu\vartheta\}$ for a given s and μ . The red Dikin ellipsoids have radius $\tau_\vartheta/(\tau_\vartheta + 1)$ and contain the points \hat{x}_i . The black curves show the boundary of the neighborhood $\gamma_G \leq 1/(\tau_\vartheta + 1)$ and the blue curves show the boundary of the region $\gamma_\infty \leq 1/\tau_\vartheta$.

If we denote the eigenvalues of xs in these expressions by v_i , and apply (43) in Theorem 4.3, we obtain

$$\frac{1}{\check{\xi}_F} = \inf_{v \in \mathbb{R}_{++}^m} \left((\min_i v_i) \left(\sum_{j=1}^m \frac{1}{v_j} - \frac{m(m-1)}{\sum_{j=1}^m v_j} \right) \right).$$

The rest of the proof follows as in the proof of Theorem 4.4. The statement about the Nesterov–Todd scaling and the integral scaling also follow from Theorem 4.3. \square

Figure 3 (left) shows the cone \mathbb{S}_+^2 intersected with a hyperplane $\{x \in \mathbb{S}_+^2 : \text{Tr}(sx) = 2\mu\}$, for a given positive definite s and positive μ . Three points \hat{x}_i in the plane attain $\check{\xi}_F$ together with s .

The figure on the right illustrates some of the differences between self-scaled barriers and LHSCBs with negative curvature. It shows the $m \times m$ tridiagonal positive semidefinite Toeplitz cone (with $m = 5$), intersected with the hyperplane $\{x : \langle s, x \rangle = m\mu\}$ for a fixed $s \in \text{int}(K^*)$ and μ . The barrier is the standard log-det barrier with $\vartheta = m$, i.e., of the form $F(x) = -\ln \det(A_0 + x_1 A_1 + x_2 A_2 + x_3 A_3)$ for some symmetric $m \times m$ matrices A_0, A_1, A_2, A_3 . This barrier has negative curvature but it is not self-scaled. Two points \hat{x}_1, \hat{x}_2 attain $\check{\xi}_F$ together with s . These points were determined numerically. In the two figures we also show the boundaries of three neighbourhoods: the Dikin ellipsoid with radius $\tau_\vartheta/(\tau_\vartheta + 1)$, the γ_G -neighbourhood with radius $1/(\vartheta + 1)$, and the γ_∞ -neighbourhood with radius $1/\vartheta$. In the example on the right,

$$\check{\xi}_F < \frac{\gamma_\infty(\hat{x}_i, s) + 1}{\gamma_G(\hat{x}_i, s) + 1} < \rho_\vartheta.$$

We also note that the worst-case points \hat{x}_1, \hat{x}_2 lie on the boundary of the Dikin ellipsoid with radius $\tau_\vartheta/(\tau_\vartheta + 1)$. This will be further investigated in Section 5.

4.4. Second order cone. Next, we apply Theorem 4.3 to the logarithmic barrier for the second order cone and direct sums of second order cones. For the second order cone $K = K^* = \mathcal{Q}_p :=$

$\{(y, t) \in \mathbb{R}^p \oplus \mathbb{R} : \|y\|_2 \leq t\}$, the barrier

$$F(y, t) := \begin{cases} -\ln(t^2 - y^\top y) & \text{if } (y, t) \in \text{int}(\mathcal{Q}_p); \\ +\infty, & \text{otherwise,} \end{cases} \quad (52)$$

and the corresponding dual barrier

$$F_*(w, r) := \begin{cases} -\ln(r^2 - w^\top w) - 2 & \text{if } (w, r) \in \text{int}(\mathcal{Q}_p); \\ +\infty, & \text{otherwise,} \end{cases}$$

are self-scaled with $\vartheta = 2$. Here, the dual cone and dual barrier are defined with respect to the Euclidean inner product $\langle s, x \rangle := s^\top x$. If K is the direct sum of m second order cones for some positive integer m , then the barrier

$$F(y_1, t_1, \dots, y_m, t_m) := \begin{cases} -\sum_{i=1}^m \ln(t_i^2 - y_i^\top y_i) & \text{if } (y_i, t_i) \in \text{int}(\mathcal{Q}_p), i \in \{1, \dots, m\}; \\ +\infty, & \text{otherwise,} \end{cases} \quad (53)$$

is self-scaled with $\vartheta = 2m$.

Theorem 4.7. *Let F be the barrier function (53). Then $\xi_F = \check{\xi}_F = \rho_{2m}$. Moreover, the Nesterov–Todd scaling and integral scaling at x, s are in $\mathcal{T}(x, s; \xi_F)$.*

The proof is along the lines of the proofs of Theorems 4.4 and 4.6.

4.5. General symmetric cones. The results in the previous sections generalize to all symmetric cones and optimal self-scaled barriers. This can be shown by extending the proof of Theorem 4.4 using the general theory of self-scaled barriers and Euclidean Jordan algebras [1, 7–9, 12, 19, 20, 25–27, 31, 34]. In particular, Hauser and Güler have proved the following classification result for self-scaled barriers [12, Theorem 5.5]. Let $K = K_1 \oplus \dots \oplus K_m$ be a symmetric cone, decomposed into irreducible symmetric components K_1, \dots, K_m . Then all self-scaled barriers for K can be expressed as

$$F(x_1, \dots, x_m) = \begin{cases} c_0 - \sum_{i=1}^m c_i \ln \det_{K_i}(x_i), & x_i \in \text{int}(K_i), i \in \{1, \dots, m\}; \\ +\infty, & \text{otherwise,} \end{cases} \quad (54)$$

where $c_i \geq 1$ for $i \in \{1, \dots, m\}$, and $\det_{K_i}(x_i)$ is the determinant of x_i in the Jordan algebra associated with K_i . The logarithmic homogeneity parameter for (54) is equal to $\vartheta := c_1 r_1 + \dots + c_m r_m$, where r_i is the rank of the Jordan algebra associated with K_i . The self-scaled barrier F defined in (54) is *optimal* if and only if $c_i = 1$ for all $i \in \{1, \dots, m\}$. For an optimal self-scaled barrier $\vartheta = r_1 + \dots + r_m$, the rank of the cone K ; see [11].

Theorem 4.8. *Let F be an optimal self-scaled barrier for a symmetric cone K , with rank $\vartheta \geq 2$. Then $\xi_F = \check{\xi}_F = \rho_\vartheta$. Moreover, the Nesterov–Todd scaling and the integral scaling at x, s are in $\mathcal{T}(x, s; \xi_F)$.*

We omit a detailed proof, which requires extensive preliminaries from the theory of symmetric cones and Euclidean Jordan algebras. Briefly, the key observation is that for every $x \in \text{int}(K)$ and $s \in \text{int}(K^*)$,

$$\sigma_x(\tilde{x}) = \min_{i \in \{1, \dots, \vartheta\}} v_i, \quad \delta_F(x, s) = \sum_{i=1}^{\vartheta} \frac{1}{v_i} - \frac{\vartheta(\vartheta - 1)}{\sum_{i=1}^{\vartheta} v_i},$$

where v_i , for $i \in \{1, \dots, \vartheta\}$, are the eigenvalues of $P(s^{1/2})x$ and P is the quadratic representation of the Jordan algebra associated with K (see [7, chapter 2] for the definitions of eigenvalues, square root, and quadratic representation). Substituting these expressions in (43) shows that $1/\hat{\xi}_F$ is the solution of the same optimization problem (48) as in the proof of Theorem 4.4 (with n replaced with ϑ). The last statement in the theorem was proved in Theorem 4.3.

Note the condition in Theorem 4.8 that F is an *optimal* self-scaled barrier. As an example of a non-optimal self-scaled barrier, consider $F(x_1, x_2) := -2 \ln x_1 - 2 \ln x_2$ for $K := \mathbb{R}_+^2$, and the corresponding dual barrier $F_*(s_1, s_2) = -2 \ln s_1 - 2 \ln(s_2) - 4$. The barrier F is self-scaled with $\vartheta = 4$, but not optimal. In the expression (43) for ξ_F we have $\tilde{x} = (2/s_1, 2/s_2)$,

$$\sigma_x(\tilde{x}) = \frac{2}{\min\{x_1 s_1, x_2 s_2\}}, \quad \delta_F(x, s) = \frac{4}{x_1 s_1} + \frac{4}{x_2 s_2} - \frac{\vartheta(\vartheta - 1)}{x_1 s_1 + x_2 s_2}.$$

Hence, if we define $v_i = x_i s_i$,

$$\frac{1}{\xi_F} = \inf_{v_1, v_2 > 0} \frac{\min\{v_1, v_2\}}{2} \left(\frac{4}{v_1} + \frac{4}{v_2} - \frac{\vartheta(\vartheta - 1)}{v_1 + v_2} \right) = \inf_{v_1 \geq 1} \left(\frac{2}{v_1} + 2 - \frac{\vartheta(\vartheta - 1)}{2(v_1 + 1)} \right).$$

This gives $\xi_F = 1.0774 < \rho_\vartheta = 1.2071$.

5. GENERAL LOGARITHMICALLY HOMOGENEOUS SELF-CONCORDANT BARRIERS

In Section 3 an upper bound on ξ_F was derived for LHSCBs with negative curvature (Theorem 3.6). In this section, we present bounds that apply to all LHSCBs. We also include examples in which the solution of the optimization problem in the definition of $\check{\xi}_F$ in (34) is examined numerically.

5.1. Bounds on $\check{\xi}_F$. In Section 3, the upper bound $4/3$ on $\check{\xi}_F$ and ξ_F was proved for negative curvature LHSCBs. The proof was based on Proposition 3.3. In this section, we relax the negative curvature assumption. Instead of Proposition 3.3, we have a more generally applicable, but relatively (and somewhat significantly) weaker conclusion in Proposition 5.2.

Proposition 5.1. [21, Corollary 1.3] *Let F be a ϑ -LHSCB for K , and $x, u \in \text{int}(K)$ such that $\langle F'(x), u - x \rangle \geq 0$. Then, $F''(x) \leq 4\vartheta^2 F''(u)$.*

Using the above, we conclude the following.

Proposition 5.2. *Let F be a ϑ -LHSCB for K , and $x \in \text{int}(K)$ and $s \in \text{int}(K^*)$. Then,*

$$\frac{1}{4\vartheta^2 \mu^2} F''(\tilde{x}) \leq F''(x) \leq 4\vartheta^2 \tilde{\mu}^2 F''(\tilde{x}).$$

Proof. Define $u := \tilde{x}/\tilde{\mu}$. Then $\langle F'(x), u - x \rangle = (\vartheta\tilde{\mu})/\tilde{\mu} - \vartheta = 0$ and, by Proposition 5.1, $F''(x) \leq 4\vartheta^2 F''(-F'(s)/\tilde{\mu})$. This proves the right-hand-side inequality in the statement. Next, define $u := x/\mu \in \text{int}(K)$. Then $\langle F'(\tilde{x}), u - x \rangle = (\vartheta\mu)/\mu - \vartheta = 0$ and, again by Proposition 5.1, $F''(\tilde{x}) \leq 4\vartheta^2 F''(x/\mu)$ proving the other inequality in the statement. \square

Another ingredient we need in this section is next.

Lemma 5.3. *Let F be a ϑ -LHSCB for K . Then, for every $x \in \text{int}(K)$ and for every $u \in K$, we have*

$$\langle -F'(x), u \rangle \leq \sqrt{\vartheta} \|u\|_x \leq \sqrt{\vartheta} \langle -F'(x), u \rangle.$$

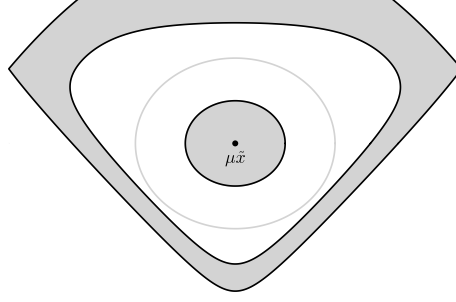


FIGURE 4. A slice of the cone of positive semidefinite tridiagonal Toeplitz matrices. The boundary of the unit Dikin ellipsoid is drawn in gray. The half Dikin ellipsoid, where it is known that $\check{\xi}_F(x, s) \leq 3$, is shaded. The region defined by $\mu\tilde{\mu} \geq 2$, where $\check{\xi}_F(x, s) \leq 4$ (see Theorem 5.4) is also shaded.

Proof. The left-hand inequality follows from $\langle F'(x), F''(x)^{-1}F'(x) \rangle = \vartheta$ and the Cauchy–Schwarz inequality. The right-hand-side is Corollary 2.3.1 in [18] (alternatively, see Theorem 1.1 in [21] or Theorem 5.1.14 in [17]). \square

Theorem 5.4. *Let F be a ϑ -LHSCB for K . Then, for every pair $(x, s) \in \text{int}(K) \oplus \text{int}(K^*)$ we have*

$$\frac{\lambda_{\max}^{1/2}(F''(x)F''(s))}{\delta_F(x, s)} \leq 2 + \frac{2(\vartheta - 1)}{\vartheta(\mu\tilde{\mu} - 1) + 1} = 2 + \frac{2(\vartheta - 1)}{\gamma_G(x, s) + 1}. \quad (55)$$

Therefore, $\check{\xi}_F \leq 2\vartheta$. Moreover, every pair (x, s) for which $\mu\tilde{\mu} \geq 2$ satisfies

$$\frac{\lambda_{\max}^{1/2}(F''(x)F''(s))}{\delta_F(x, s)} \leq 4. \quad (56)$$

Proof. Let K , F and the pair (x, s) be given as in the assumptions of the statement. We apply Proposition 5.2 and deduce

$$\frac{\lambda_{\max}^{1/2}(F''(x)F''(s))}{\delta_F(x, s)} \leq \frac{2\vartheta\mu\tilde{\mu}}{1 + \vartheta(\mu\tilde{\mu} - 1)} = 2 + \frac{2(\vartheta - 1)}{\vartheta(\mu\tilde{\mu} - 1) + 1}.$$

Since $\mu\tilde{\mu} \geq 1$ for every primal–dual interior pair, the bound $\check{\xi}_F \leq 2\vartheta$ follows. If $\mu\tilde{\mu} \geq 2$, the right-hand side of (55) is maximized by the smallest value of $\mu\tilde{\mu}$, and (56) follows. \square

5.2. Local $\check{\xi}_F$ and ξ_F . Note that the neighbourhood defined by the condition $\mu\tilde{\mu} \leq 2$ or, equivalently, $\gamma_G(x, s) \leq \vartheta$ (mentioned in Theorem 5.4) is much larger than the one defined by the Dikin ellipsoid. Moreover, the boundary of the $\mu\tilde{\mu} \leq 2$ neighborhood approximates the shape of the feasible region much better than the Dikin ellipsoid. For an illustration, see Figure 4. These considerations motivate us to look at the complexity measure $\check{\xi}_F$ locally. We define

$$\check{\xi}_F(x, s) := \frac{\lambda_{\max}^{1/2}(F''(x)F''(s))}{\delta_F(x, s)}.$$

This is the smallest ξ for which $\check{\mathcal{T}}(x, s; \xi)$ is not empty. Similarly, we define $\xi_F(x, s)$ as the smallest ξ for which $\mathcal{T}(x, s; \xi)$ is not empty. (With these definitions, $\check{\xi}_F = \sup_{x,s} \check{\xi}_F(x, s)$ and $\xi_F = \sup_{x,s} \xi_F(x, s)$.) In the proof of Theorem 4.3 we showed that for self-scaled barriers F and every pair of interior points x, s , the Nesterov–Todd scaling is in $\mathcal{T}(x, s; \xi)$ for $\xi = \xi_F(x, s)$, so it is optimal for the local measure $\xi_F(x, s)$ as well as for the global measure ξ_F . The following list summarizes properties of the local complexity measure for ϑ -LHSCBs F .

- $\xi_F(x, s) < 1.2115$ for all (x, s) in a small neighborhood of the central path [14, Theorem 6.8].
- $\xi_F(x, s) \leq 3$ for all (x, s) such that $\mu\tilde{\mu}$ lies in the Dikin ellipsoid with radius $1/2$ centered at x [22, Section 8.1].
- $\check{\xi}_F(x, s) \leq 4$ for all (x, s) such that $\mu\tilde{\mu} \geq 2$ (Theorem 5.4).

5.3. Worst-case primal–dual pairs. To gain more insight in the complexity measures ξ_F and $\check{\xi}_F$, we now examine the optimization problem in the definition of $\check{\xi}_F$. Using the Rayleigh-Ritz characterization of the maximum eigenvalue in (34), we can express $\check{\xi}_F$ in the following variational form:

$$\check{\xi}_F^{-1} = \inf_{(x,s) \in \text{int}(K) \oplus \text{int}(K^*), v \in \mathbb{R}^n \setminus \{0\}} \sqrt{R(x, s, v)} \cdot \delta_F(x, s), \quad (57)$$

where

$$R(x, s, v) := \frac{\langle F''_*(s)^{-1}v, v \rangle}{\langle F''(x)v, v \rangle}.$$

The worst-case primal–dual pairs (x, s) are pairs that are optimal for the minimization problem in (57).

In Figures 2 and 3, and the examples later in the section, it can be noted that the worst-case points \hat{x}_i appear to have additional geometric properties related to the next proposition.

Proposition 5.5. *Consider the optimization problem*

$$\begin{aligned} & \text{maximize} && \langle F''(\tilde{x})v, v \rangle \\ & \text{subject to} && \langle s, v \rangle = \mu\vartheta \\ & && v \in K, \end{aligned} \quad (58)$$

with variable v , where $\mu = \langle s, x \rangle / \vartheta$ and $x \in \text{int}(K)$ and $s \in \text{int}(K^*)$ are given. Suppose v is feasible in (58) and satisfies $\|v - \mu\tilde{x}\|_{\mu\tilde{x}}^2 = \vartheta(\vartheta - 1)$. Then v is optimal. Furthermore, the point

$$r := \tau_\vartheta(s - \frac{1}{\mu\vartheta}F''(\tilde{x})v) \quad (59)$$

is in K^* , and the point

$$\hat{x} := (1 - \tau_\vartheta)v + \tau_\vartheta\mu\tilde{x} \quad (60)$$

satisfies $\hat{x} \in \text{int}(K)$, $\langle s, \hat{x} \rangle = \mu\vartheta$, and $\|\hat{x} - \mu\tilde{x}\|_{\mu\tilde{x}} = \tau_\vartheta / (\tau_\vartheta + 1)$.

Proof. We first note that the optimal value of (58) is bounded above by $(\vartheta\mu)^2$: from Lemma 5.3,

$$\|v\|_{\tilde{x}} \leq \langle -F'(\tilde{x}), v \rangle = \langle s, v \rangle = \vartheta\mu$$

holds for any feasible v . Hence, for any feasible v ,

$$\|v - \mu\tilde{x}\|_{\mu\tilde{x}}^2 = \frac{1}{\mu^2}\|v\|_{\tilde{x}}^2 + \vartheta - 2\frac{\langle s, v \rangle}{\mu} \leq \vartheta(\vartheta - 1),$$

and if equality holds, $\|v\|_{\tilde{x}} = \vartheta\mu$ and v is optimal in (58). The property $r \in K^*$ follows from the optimality conditions of (58): v is optimal if it is feasible and

$$-2F''(\tilde{x})v + \lambda s \in K^*, \quad \langle -2F''(\tilde{x})v + \lambda s, v \rangle = 0$$

for some λ . From the second condition, $\lambda = 2\mu\vartheta$ if $\|v\|_{\tilde{x}}^2 = (\vartheta\mu)^2$. The properties of \hat{x} follow from

$$\|\hat{x} - \mu\tilde{x}\|_{\mu\tilde{x}} = (\tau_\vartheta - 1)\|v - \mu\tilde{x}\|_{\mu\tilde{x}} = (\tau_\vartheta - 1)\sqrt{\vartheta(\vartheta - 1)} = \frac{\tau_\vartheta}{\tau_\vartheta + 1} < 1.$$

This shows that \hat{x} lies in the unit Dikin ellipsoid with center $\mu\tilde{x}$ and therefore $\hat{x} \in K$. Furthermore, $\langle s, \hat{x} \rangle = (1 - \tau_\vartheta)\mu\vartheta + \tau_\vartheta\mu\vartheta = \mu\vartheta$. \square

For self-scaled barriers (Figure 2 and the left-hand plot of Figure 3), the worst-case points \hat{x}_i satisfy (60) for points v that are optimal in (58) with $\|v\|_{\tilde{x}} = \mu\vartheta$ (equivalently, $\|v - \mu\tilde{x}\|_{\mu\tilde{x}}^2 = \vartheta(\vartheta - 1)$). Next, we consider some examples with general LHSCBs. In the first two examples, points v with the properties in the Proposition 5.5 exist, and corresponding points \hat{x} in (60) are worst-case points. However, as Example 5.8 shows, points v with the required property do not always exist.

Example 5.6. The exponential cone is defined as

$$K_{\text{exp}} := \text{cl}\{x \in \mathbb{R}^3 : x_1 \geq x_2 \exp(x_3/x_2), x_2 > 0\},$$

and its dual cone is

$$K_{\text{exp}}^* = \text{cl}\{z \in \mathbb{R}^3 : e \cdot z_1 \geq -z_3 \exp(z_2/z_3), z_1 > 0, z_3 < 0\}.$$

A 3-LHSCB for K_{exp} is $F(x) := -\ln(\psi(x))$, where

$$\psi(x) := x_1 x_2^2 \ln(x_1/x_2) - x_1 x_2 x_3.$$

Figure 5a shows the intersection of K_{exp} with the hyperplane $\{x \in \mathbb{R}^3 : \langle s, x \rangle = 1\}$, where $s := (1, 1, -1)$. The extreme point $v := (0, 0, -1) \in K_{\text{exp}}$ satisfies $\|v - \mu\tilde{x}\|_{\mu\tilde{x}}^2 = \vartheta(\vartheta - 1)$. The point \hat{x} defined in (60) lies on the inner Dikin ellipsoid of radius $\tau_\vartheta/(\tau_\vartheta + 1)$. It was verified numerically that (\hat{x}, s, v) satisfies the stationarity conditions for (57), and that $\check{\xi}_F(\hat{x}, s) = \rho_\vartheta$. Furthermore, $r \in K_{\text{exp}}^*$, where r is defined in (59). This point is shown in Figure 5b.

From the primal–dual symmetry in the definition of $\check{\xi}(F; \hat{x}, s)$, we can also consider worst-case pairs in the dual cone K_{exp}^* intersected with the hyperplane $\{y \in \mathbb{R}^3 : \langle y, \hat{x} \rangle = 1\}$; see Figure 5b. The points

$$u := \frac{1}{(1 - \tau_\vartheta)} (s - \tau_\vartheta \mu F'(\hat{x})), \quad t := \tau_\vartheta \left(\hat{x} - \frac{1}{\mu\vartheta} F''(\hat{x})^{-1} u \right)$$

satisfy $u \in K_{\text{exp}}^*$ and $t \in K_{\text{exp}}$, and $\|u - \mu\tilde{s}\|_{\mu\tilde{s}}^* = (\vartheta(\vartheta - 1))^{1/2}$, where $\|y\|_{\mu\tilde{s}}^* := \langle y, F''(\mu\tilde{s})y \rangle^{1/2}$. The points (s, \hat{x}, u) satisfy the stationarity conditions for (57).

As an extension we also considered a product of exponential cones $K := K_1 \oplus K_2 \oplus \dots \oplus K_n$ where each $K_i := K_{\text{exp}}$. The barrier F is the summation of the barriers for each K_i from the previous example, and has parameter $\vartheta = 3n$. Assume $s \in \text{int } K^*$. We define $v := (v_1, v_2, \dots, v_n) \in K$ where $v_k := (0, 0, \beta)$ and $v_i := (0, 0, 0)$ for $i \neq k$, and β is chosen such that $\langle s, v \rangle = \mu\vartheta$. Then

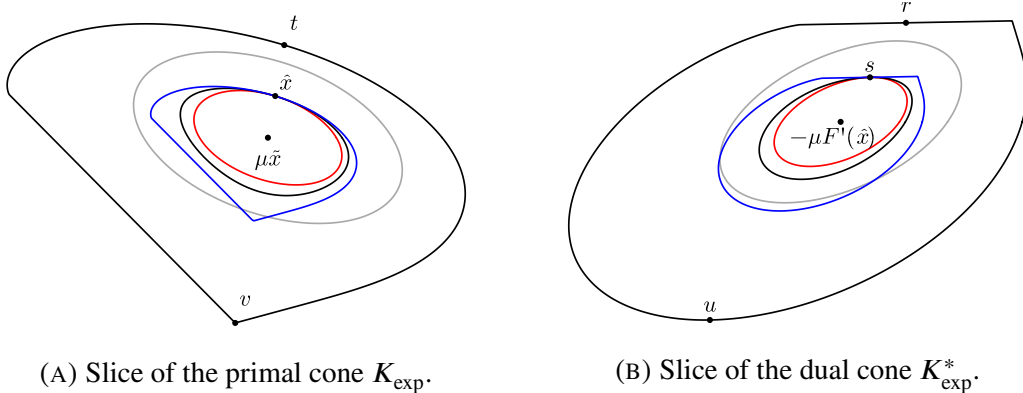


FIGURE 5. Primal and dual exponential cone intersected with the hyperplanes normal to s and \hat{x} , respectively. The inner Dikin ellipsoids (red) have radius $\tau_\vartheta/(\tau_\vartheta + 1)$ and include the pair of worst-case points \hat{x} and s . The boundary of the region $\gamma_G(x, s) \leq 1/(\tau_\vartheta + 1)$ is shown in black, and the boundary of $\gamma_\infty(x, s) \leq 1/\tau_\vartheta$ in blue. The points (v, t) and (u, r) lie on the boundaries of K_{exp} and K_{exp}^* , respectively.

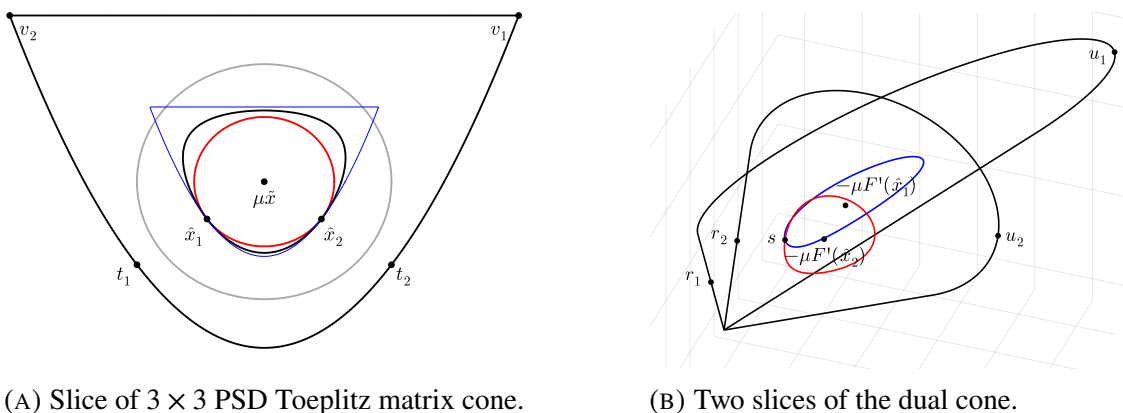


FIGURE 6. *Left.* Cone of 3×3 positive semidefinite Toeplitz matrices cone intersected with the hyperplane defined by $\text{Tr}(sx) = 1$, where s is the identity matrix. The unit Dikin ellipsoid is shown in gray. The inner Dikin ellipsoid (red) has radius $\tau_\vartheta/(\tau_\vartheta + 1)$ and includes $\hat{x}_i = (1 - \tau_\vartheta)v_i + \tau_\vartheta\mu\tilde{x}$ for $i \in \{1, 2\}$. The boundary of the region $\gamma_G(x, s) \leq 1/(\tau_\vartheta + 1)$ is shown in black, and the boundary of $\gamma_\infty(x, s) \leq 1/\tau_\vartheta$ in blue. *Right.* Dual cone intersected with the two hyperplanes $\{y \in \mathbb{R}^3 : \langle y, \hat{x}_i \rangle = \mu\vartheta\}$ for $i \in \{1, 2\}$. The smallest γ_G neighborhoods including s and centered at $-\mu F'(\hat{x}_1)$ and $-\mu F'(\hat{x}_2)$ are shown in blue and red, respectively. The two hyperplanes intersect at s .

$\|v - \mu\tilde{x}\|_{\mu\tilde{x}}^2 = \vartheta(\vartheta - 1)$. Furthermore, the point \hat{x} defined in (60) satisfies $\check{\xi}_F(\hat{x}, s) = \rho_\vartheta$ and (\hat{x}, s, v) satisfies the stationarity assumptions for (57).

Example 5.7. We consider the cone of 3×3 positive semidefinite Toeplitz matrices with the standard 3-LHSCB log-det barrier. Figure 6a shows the intersection of the cone with the hyperplane defined by $\text{Tr}(sx) = 1$, where s is the identity matrix. The two extreme points are the matrices

$$v_1 := \begin{bmatrix} 1 & 1 & 1 \\ 1 & 1 & 1 \\ 1 & 1 & 1 \end{bmatrix}, \quad v_2 := \begin{bmatrix} 1 & -1 & 1 \\ -1 & 1 & -1 \\ 1 & -1 & 1 \end{bmatrix},$$

and satisfy $\|v_1 - \mu\tilde{x}\|_{\mu\tilde{x}} = \|v_2 - \mu\tilde{x}\|_{\mu\tilde{x}} = (\vartheta(\vartheta-1))^{1/2}$. The two stationary points on the inner Dikin ellipsoid are given by $\hat{x}_i = (1 - \tau_\vartheta)v_i + \tau_\vartheta\mu\tilde{x}$ and satisfy $\check{\xi}_F(\hat{x}_i, s) = \rho_\vartheta$ as well as the stationarity assumptions for (57).

Figure 6b shows K^* intersected by the two hyperplanes normal to \hat{x}_1 and \hat{x}_2 , respectively. The points in the figure are defined as

$$u_i := \frac{1}{(1 - \tau_\vartheta)} (s - \tau_\vartheta\mu F'(\hat{x}_i)), \quad t_i := \tau_\vartheta \left(\hat{x}_i - \frac{1}{\mu\vartheta} F''(\hat{x}_i)^{-1} u \right), \quad i \in \{1, 2\},$$

and satisfy the conditions for (57). Points $t_i \in K$ are shown in Figure 6a. The points r_i are defined as

$$r_i := \tau_\vartheta \left(s - \frac{1}{\mu\vartheta} F''(\tilde{x})v_i \right), \quad i \in \{1, 2\}.$$

Example 5.8. We consider the cone of 5×5 positive semidefinite tridiagonal Toeplitz matrices, with the standard 5-LHSCB log-det barrier. Figure 3 shows the intersection of the cone with a hyperplane normal to the identity matrix. For this example, all points $v \in K$ on the hyperplane have $\|v - \mu\tilde{x}\|_{\mu\tilde{x}}^2 < \vartheta(\vartheta-1)$, and there are no points $\hat{x} \in K$ on the hyperplane satisfying $\check{\xi}_F(\hat{x}, s) = \rho_\vartheta$.

6. CONCLUSION

We showed that $\xi_F \leq 4/3$ for all LHSCBs with negative curvature and that the integral scaling is an element of $\mathcal{T}(x, s; 4/3)$. An immediate consequence of this result is that the primal–dual potential reduction algorithm from [36] when implemented using the integral primal–dual scalings [14] has iteration complexity $O(\vartheta^{1/2} \ln(1/\epsilon))$. This result positively impacts other primal–dual algorithms, e.g., the predictor–corrector algorithm analyzed in [14]. For negative curvature barriers, our results imply that in primal–dual predictor–corrector algorithms, implemented with the integral scaling (or its suitable approximations), we may take significantly larger predictor steps and still maintain $O(\vartheta^{1/2} \ln(1/\epsilon))$ iteration complexity bounds.

Our result on negative curvature barriers covers a large class of convex cones including hyperbolicity cones arising from hyperbolic polynomials. However, the following problems remain open:

- (1) For every LHSCB F , characterize the pairs (x, s) attaining the value $\check{\xi}_F$.
- (2) For every LHSCB F , characterize the pairs (x, s) attaining the value ξ_F .
- (3) Does every convex cone admit an LHSCB with negative curvature?
- (4) Does every convex cone admit an LHSCB F with $\xi_F \leq 4/3$?

Question (3) was originally posed in [21]. If the answer to question (3) is “yes,” then our results imply that the answer to question (4) is also “yes.”

Another line of related future research concerns the investigation of characterizations of worst-case pairs (x, s) (i.e., those which satisfy $\check{\xi}_F(x, s) = \xi_F$) with respect to the properties of the barrier F and the geometry of K as suggested by many of the figures in the paper.

REFERENCES

- [1] Farid Alizadeh and Donald Goldfarb. Second-order cone programming. *Mathematical Programming Series B*, 95:3–51, 2003.
- [2] Erling D Andersen, Kees Roos, and Tamas Terlaky. On implementing a primal-dual interior-point method for conic quadratic optimization. *Mathematical Programming*, 95:249–277, 2003.
- [3] Martin S. Andersen, Joachim Dahl, and Lieven Vandenbergh. Implementation of nonsymmetric interior-point methods for linear optimization over sparse matrix cones. *Mathematical Programming Computation*, 2(3):167–201, 2010.
- [4] Riley Badenbroek and Joachim Dahl. An algorithm for nonsymmetric conic optimization inspired by MOSEK. *Optim. Methods Softw.*, 37(3):1027–1064, 2022.
- [5] Yuwen Chen and Paul Goulart. An efficient implementation of interior-point methods for a class of nonsymmetric cones. *Journal of Optimization Theory and Applications*, 204(2):1–28, 2025.
- [6] Joachim Dahl and Erling D. Andersen. A primal-dual interior-point algorithm for nonsymmetric exponential-cone optimization. *Math. Program.*, 194(1-2):341–370, 2022.
- [7] Jacques Faraut and Adam Korányi. *Analysis on Symmetric Cones*. Oxford university press, 1994.
- [8] Leonid Faybusovich. Euclidean Jordan algebras and interior-point algorithms. *Positivity*, 1(4):331–357, 1997.
- [9] Leonid Faybusovich. Linear systems in Jordan algebras and primal-dual interior-point algorithms. *Journal of computational and applied mathematics*, 86(1):149–175, 1997.
- [10] Osman Güler. Hyperbolic polynomials and interior point methods for convex programming. *Math. Oper. Res.*, 22(2):350–377, 1997.
- [11] Osman Güler and Levent Tunçel. Characterization of the barrier parameter of homogeneous convex cones. *Math. Programming*, 81(1, Ser. A):55–76, 1998.
- [12] Raphael A. Hauser and Osman Güler. Self-scaled barrier functions on symmetric cones and their classification. *Found. Comput. Math.*, 2(2):121–143, 2002.
- [13] Mehdi Karimi and Levent Tunçel. Primal-dual interior-point methods for domain-driven formulations. *Math. Oper. Res.*, 45(2):591–621, 2020.
- [14] Tor G. J. Myklebust and Levent Tunçel. Interior-point algorithms for convex optimization based on primal-dual metrics. *arXiv preprint arXiv:1411.2129*, 2014.
- [15] Arkadi Nemirovski and Levent Tunçel. “Cone-free” primal-dual path-following and potential-reduction polynomial time interior-point methods. *Math. Program.*, 102(2):261–294, 2005.
- [16] Yurii Nesterov. Towards non-symmetric conic optimization. *Optim. Methods Softw.*, 27(4-5):893–917, 2012.
- [17] Yurii Nesterov. *Lectures on convex optimization*, volume 137 of *Springer Optimization and Its Applications*. Springer, 2018.
- [18] Yurii Nesterov and Arkadii Nemirovskii. *Interior-point polynomial algorithms in convex programming*, volume 13 of *SIAM Studies in Applied Mathematics*. Society for Industrial and Applied Mathematics (SIAM), Philadelphia, PA, 1994.
- [19] Yurii Nesterov and Michael J. Todd. Self-scaled barriers and interior-point methods for convex programming. *Math. Oper. Res.*, 22(1):1–42, 1997.
- [20] Yurii Nesterov and Michael J. Todd. Primal-dual interior-point methods for self-scaled cones. *SIAM J. Optim.*, 8(2):324–364, 1998.
- [21] Yurii Nesterov and Levent Tunçel. Local superlinear convergence of polynomial-time interior-point methods for hyperbolicity cone optimization problems. *SIAM J. Optim.*, 26(1):139–170, 2016.
- [22] Mikkel Øbro. Conic optimization with exponential cones. Master’s thesis, DTU, Denmark, 2019.
- [23] Dávid Papp and Sercan Yıldız. Alfonso: Matlab package for nonsymmetric conic optimization. *INFORMS Journal on Computing*, 34(1):11–19, 2022.
- [24] James Renegar. *A mathematical view of interior-point methods in convex optimization*. MPS/SIAM Series on Optimization. Society for Industrial and Applied Mathematics (SIAM), Philadelphia, PA; Mathematical Programming Society (MPS), Philadelphia, PA, 2001.
- [25] S. H. Schmieta and F. Alizadeh. Extension of primal-dual interior point algorithms to symmetric cones. *Mathematical Programming*, 96:409–438, 2003.
- [26] S. H. Schmieta and Farid Alizadeh. Associative and Jordan algebras, and polynomial time interior-point algorithms for symmetric cones. *Mathematics of Operations Research*, 26(3):543–564, 2001.

- [27] Stefan H. Schmieta. Complete classification of self-scaled barrier functions. Technical report, Department of IEOR, Columbia University, 2000.
- [28] Santiago Akle Serrano. *Algorithms for unsymmetric cone optimization and an implementation for problems with the exponential cone*. PhD thesis, Stanford University, 2015.
- [29] Anders Skajaa and Yinyu Ye. A homogeneous interior-point algorithm for nonsymmetric convex conic optimization. *Math. Program.*, 150(2):391–422, 2015.
- [30] Jos F. Sturm. Using SeDuMi 1.02, a MATLAB toolbox for optimization over symmetric cones. *Optim. Methods Softw.*, 11/12(1-4):625–653, 1999. Interior point methods.
- [31] Jos F. Sturm. Similarity and other spectral relations for symmetric cones. *Linear Algebra and its applications*, 312(1-3):135–154, 2000.
- [32] Michael J. Todd. Semidefinite optimization. *Acta Numer.*, 10:515–560, 2001.
- [33] Kim-Chuan Toh, Michael J. Todd, and Reha H. Tütüncü. On the implementation and usage of SDPT3—a Matlab software package for semidefinite-quadratic-linear programming, version 4.0. In *Handbook on semidefinite, conic and polynomial optimization*, volume 166 of *Internat. Ser. Oper. Res. Management Sci.*, pages 715–754. Springer, New York, 2012.
- [34] Levent Tunçel. Primal-dual symmetry and scale invariance of interior-point algorithms for convex optimization. *Math. Oper. Res.*, 23(3):708–718, 1998.
- [35] Levent Tunçel and Lieven Vandenbergh. Linear optimization over homogeneous matrix cones. *Acta Numer.*, 32:675–747, 2023.
- [36] Levent Tunçel. Generalization of primal-dual interior-point methods to convex optimization problems in conic form. *Found. Comput. Math.*, 1(3):229–254, 2001.
- [37] Stephen J. Wright. *Primal-Dual Interior-Point Methods*. SIAM, Philadelphia, 1997.